Fizika Nizkikh Temperatur 1996, v. 22, No 3, p. 231–242

# Superconducting properties of fullerenes in the mixed state

**(Review Article)**

V. Buntar and H. W. Weber

*Atominstitut der Österreichischen Universitäten, Schüttelstr. 115, A-1020 Wien, Austria*

Submitted July 25, 1995, resubmitted September 12, 1995

A review of magnetization measurements and their evaluation in terms of critical fields and characteristic lengths in fullerene superconductors is presented. Typical results of magnetization curves are shown and the evaluation of the superconducting fraction from these measurements is discussed. We also discuss results on determination of the critical fields and characteristic lengths by different experimental techniques and make a comparison of these results between granular and crystalline samples.

Contents



## Introduction

Using a laser evaporation technique Rohlfing et al. [1] showed in 1984 for the first time that carbon clusters $C_n$ with a large number of atoms (up to $n = 190$) could be produced. Mass spectrometry [1] indicated that the peaks of $C_n$ clusters with $n$ from 40 to 190 were not very strong and of roughly equal peak height. Shortly later, Kroto et al. [2] demonstrated that the $C_{60}$ peak could be increased by a factor of 40 compared to neighboring mass peaks by increasing the time between evaporation and expansion and by increasing the helium pressure during the laser pulse. The authors suggested that $C_{60}$ was the most stable cluster, which consisted of 20 hexagons and 12 pentagons and had a shape very similar to the shape of a soccer ball. In honour of the architect Buckminster Fuller, who built similar structures consisting of pentagons and hexagons, the so-called «geodesic domes», the $C_n$ clusters were called «buckminsterfullerenes» or, later, fullerenes. At that time, they were considered to be an exotic species of material. Five years later, Krätschmer et al. [3] discovered a method to separate fullerenes from carbon in experimentally obtained carbon soot. This work showed an easy way to obtain sufficient quantities of fullerenes for experimental investigations and led to intensive investigations of this new (fourth) form of solid carbon.

During the last five years, fullerenes have attracted interest from scientists in different areas such as chemistry, physics, biology, etc. From the point of view of solid state physics, pure fullerenes and fullerene based compounds are interesting because of their molecular structure and their intriguing structural, dynamic (see, for instance, Refs. 4–14), magnetic (Refs. 15, 16) and electronic properties in the solid state [4].

Conductivity [17] and superconductivity [18,19] of the alkali-metal doped fullerenes were discovered less than one year after the production method for bulk quantities of $C_{60}$ and $C_{70}$ had been published [3]. The phenomenon of superconductivity is one of the most fascinating properties of «the roundest of all round molecules» [20], which attracted enormous scientific interest in this new form of carbon. In many aspects the situation was similar to that shortly after the discovery of superconductivity at high temperatures in the copper oxides [21,22]. Fullerene superconductors were the second group of materials besides the

cuprates, which overcame the previous boundary for the critical temperatures, $T_c = 23.2$ K ($Nb_3Ge$), in conventional superconductors. More than twenty superconducting compounds of doped fullerenes have been synthesised by now. The highest critical temperature ($T_c = 40$ K) occurs in the fullerene $Cs_3C_{60}$ [23]. These new superconducting compounds can be prepared easily by heating alkali metal — $C_{60}$ mixtures at $T = 300$ °C or by keeping $C_{60}$ in an alkali metal vapor atmosphere. However, to get from the synthesis of individual samples to practical applications of these superconductors, numerous investigations of the physical properties, stability, reproducibility, and the elaboration of technologies for the production of large quantities for technical use are required. One of the biggest problems is their instability against air. It is enough to expose the superconductor to air for a fraction of a second to completely destroy superconductivity. However, we believe that this main barrier can be overcome and that a knowledge of all of the superconducting parameters is the most important goal at the moment.

Numerous experimental investigations of these superconductors, both in granular and in crystalline form, show unique properties and distinguish them from other superconducting materials. It was shown (see, for instance, Ref. 24), that superconductivity in alkali-metal doped fullerenes occurs in the face-centered-cubic (fcc) crystal phase with the composition $A_xB_{3-x}C_{60}$ [25]. The other crystalline phases, such as body-centered-cubic (bcc) and body-centered-tetragonal (bct), do not show superconductivity. In the other family of fullerene superconductors, alkali-earth-doped $C_{60}$, superconductivity occurs in bcc $Ba_6C_{60}$ [26], $Sr_6C_{60}$ [24] and in simple cubic $Ca_5C_{60}$ [27].

One of the most important results is the experimentally established empirical linear correlation of the transition temperature $T_c$, both with the lattice constant of the cubic structure $a$ [25, 28–30] and with the density of states at the Fermi level [31–33]. It was shown that the slope of this $T_c(a)$ linear relation depended on the degree of orientational order of the fullerene molecules [34–36]. Very recently [37], a second, much steeper $T_c(a)$ dependence was found for the space group $Pa\bar{3}$ [38], which could lead to much higher $T_c$'s, if only a slight increase in $a$ could be achieved (Fig. 1).

An enormous number of results on fullerene superconductivity is being discovered every day and even during writing this short review. It is almost impossible to overview all of them. In the present contribution we shall not discuss current results on the mechanism of fullerene superconductivity, on the pairing mechanism in these materials and on the question whether the metallic $A_xC_{60}$ phases are conventional metals or manifest strong correlation effects. This discussion can be found in a recent theoretical review by Gelfand [39]. Also, we shall not discuss here the structural investigations of different groups of fullerene superconductors. We restrict ourselves to their magnetic properties. After presenting typical results of magnetization curves in Sec. 1, the evaluation of the critical fields and the characteristic lengths will be discussed in Sec. 2. Finally, a summary of the present experimental situation will be given in Sec. 3.

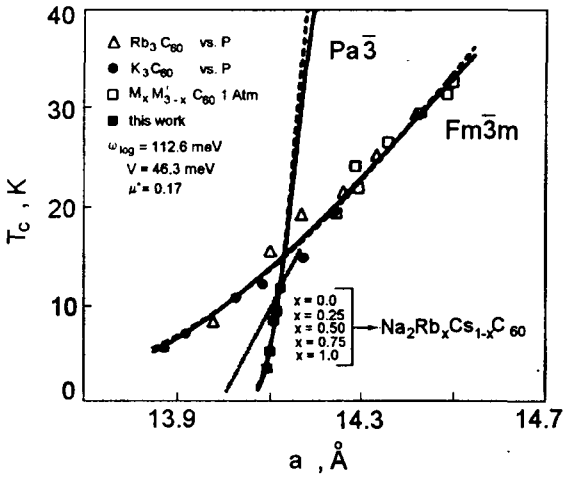


*Fig. 1.* $T_c$ versus $a$ for $Fm3m$ [29–30] and $Pa3$-ordered superconductors [38]. Solid and dashed lines are fits to McMillan's formula using linear and power law dependences, respectively, of $N(E_F)$ on the intermolecular distance; only the parameters describing $N(E_F)$ vs. $a$ differ in the fits for the two families of materials. The slope of the $Pa3$ curve is much larger than for $Fm3m$, indicating that a small increase in $a$ without destroying $Pa3$ ordering should cause $T_c$ to increase very rapidly. The dotted line represents the results of Ref. 90. (Reproduced from Ref. 38).

## 1. Magnetization curves

The first experiments on $K_3C_{60}$ [40] and $Rb_3C_{60}$ [41,42] established that alkali-doped fullerenes were «strong» type II superconductors and that their main superconducting parameters, the Ginzburg–Landau parameter $\kappa$, the penetration depth $\lambda$, the coherence length $\xi$, and the critical fields $H_{c1}$ and $H_{c2}$, were very similar to those of the high-$T_c$ oxides.

If a type II superconductor is subjected to a small magnetic field $H < H_{c1}$, the field is completely expelled. Shielding currents, which flow at the surface of the superconductor, prevent any penetration of flux. The superconductor is in the Meissner state and behaves like a type I superconductor. When increasing the external magnetic field, beyond the lower

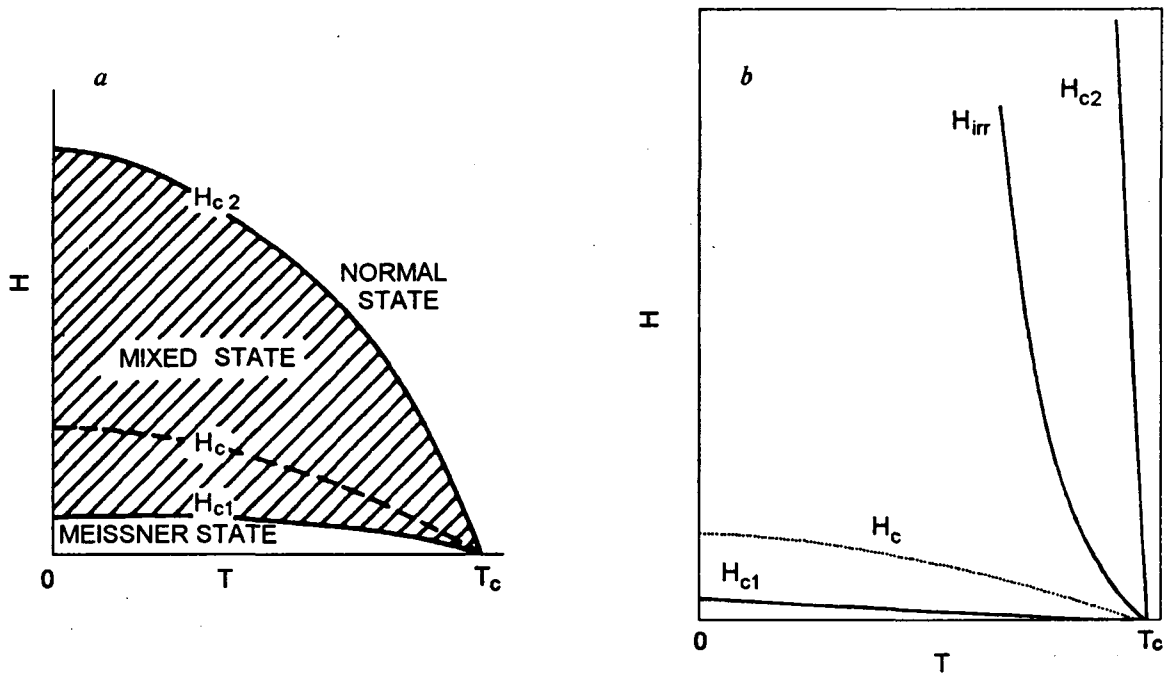


*Fig. 2.* Magnetic phase diagrams of conventional type II superconductors (*a*); fullerene superconductors (*b*).

critical field $H_{c1}$, flux penetrates the sample in the form of quantized flux lines (vortices). This happens when the vortex energy is smaller than the magnetic energy associated with the current flow shielding the superconductor. The superconductor is in the mixed state, also called the Shubnikov phase. At $H > H_{c2}$, the induction $B$ inside the sample is equal to the external field $H$ and superconductivity is completely destroyed. Type II superconductors in the mixed state ($H_{c1} < H < H_{c2}$) are no longer ideal diamagnets.

The magnetic field–temperature ($H$–$T$) diagram provides us with information on the main characteristic lengths, which can be calculated from the critical fields. Fullerene superconductors have, in principle, the same magnetic phase diagram as conventional type II superconductors (Figs. 2,*a* and 2,*b*). However, fullerenes as well as high temperature superconductors have an additional line between the lower and the upper critical fields, the irreversibility line $H_{irr}(T)$ (Fig. 2,*b*). This line separates the region where the magnetization $M$ is reversible ($H > H_{irr}$) from the region where hysteretic effects are significant. Both, the critical current density $J_c$, and $H_{irr}$ strongly depend on flux pinning.

Measurements of the magnetization in the superconducting state are usually quite straightforward and convenient for characterizing the new materials, especially powders, small crystals, fragile materials, etc., because they do not require contacts. Typical temperature and magnetic field dependences as well

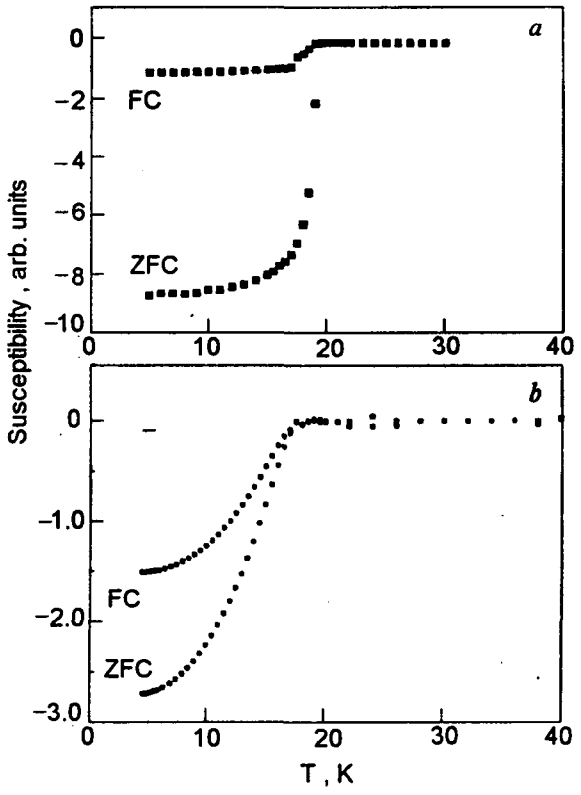


*Fig. 3.* Temperature dependence of the zero-field cooled (ZFC) and field-cooled (FC) dc magnetic susceptibility of $K_3C_{60}$ crystal (*a*) and powder (*b*) at $\mu_0 H = 1$ mT. (Fig. 3,*b* reproduced from Ref. 41).

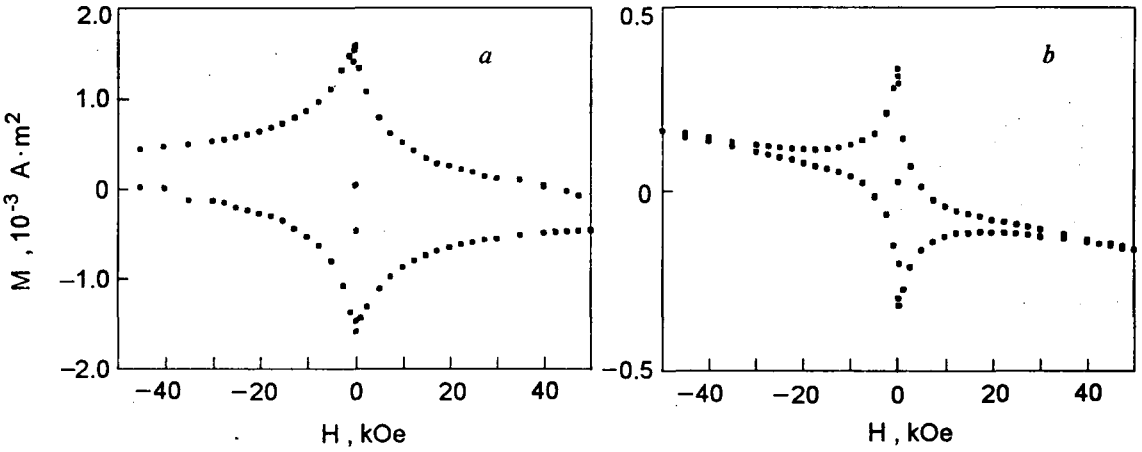


*Fig. 4.* Hysteresis loops for $Rb_3C_{60}$ powder at $T = 7$ K (*a*) and 20 K (*b*). (Reproduced from Ref. 41)

as the time relaxation of the magnetization $M$, measured for $K_3C_{60}$ and $Rb_3C_{60}$ superconductors [41] with a SQUID magnetometer, are shown in Figs. 3, 4 and in the inset on Fig. 5.

To obtain the temperature dependence of the magnetization (Fig. 3), the experiments are made as follows. The samples are cooled down to $T = 5$ K in zero external magnetic field. After temperature stabilization, a magnetic field ($\mu_0 H = 1$ mT) is applied and the magnetization monitored at increasing temperatures up to $T > T_c$. This measurement shows the shielding fraction of the sample and is called the zero-field-cooled (ZFC) curve. Then the measurement is continued at the same external magnetic field with decreasing in temperature down to $T = 5$ K. This is the field-cooled (FC) curve, which shows the Meissner effect. We wish to point out, that the ZFC magnetization shows the flux exclusion from the sample, while the FC magnetization shows the flux expulsion. A big difference between the ZFC and FC curves (Fig. 3) and a strong hysteresis in the magnetic field dependence of the magnetization at fixed temperature (Fig. 4) indicate pinning of the magnetic vortices. The fact that the FC signals of the $K_3C_{60}$ crystal (Fig 3,*a*) is very small and lies close to the zero-magnetization line, shows that pinning in the sample is extremely strong and that there is almost no expulsion of the magnetic field.

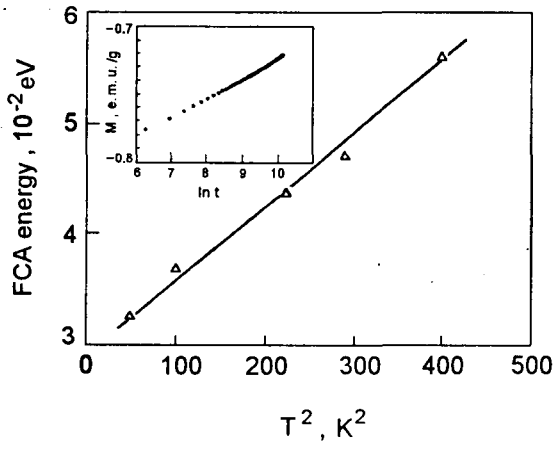


*Fig. 5.* Flux creep activation energy (FCA) vs. $T^2$ for $Rb_3C_{60}$ powder at $\mu_0 H = 1$T. Inset: example of the time decay of the magnetization at $\mu_0 H = 1$T, $T = 7$ K. (Reproduced from Ref. 41)

The magnitudes of the ZFC and FC magnetizations at the lowest temperature can be used for an evaluation of the «superconducting fraction» $X_{sc}$. Indeed, the zero-field-cooled susceptibility of a perfect superconductor should approach minus one at applied fields below the lower critical field. The Meissner effect for a perfect superconductor is shown schematically in Fig. 6,*a*. Then, the relation $\chi_{exp} \cdot 100\%$, where $\chi_{exp}$ is the experimentally obtained susceptibility, should yield $X_{sc}$. However, one should remember that the ZFC susceptibility does actually not represent exactly the superconducting fraction, but the shielding fraction. For example, if the inner part of the superconductor is not superconducting and if there is only a thin superconducting surface layer, then ZFC will exhibit full flux exclusion as for a perfect diamagnet, as is shown in Fig. 6,*b*. This effect increases the effective «superconducting fraction». On the other hand, for powdered samples with an average grain size $r$, which is of the order of or slightly bigger than the penetration depth $\lambda$, flux penetrates grains even at very small fields and this effect decreases the effective superconducting fraction (see Fig. 6,*c*). The latter is especially important for powdered fullerene samples, which usually have $r \sim 1\,\mu$m and $\lambda \sim 300$ nm. The influence of granula-

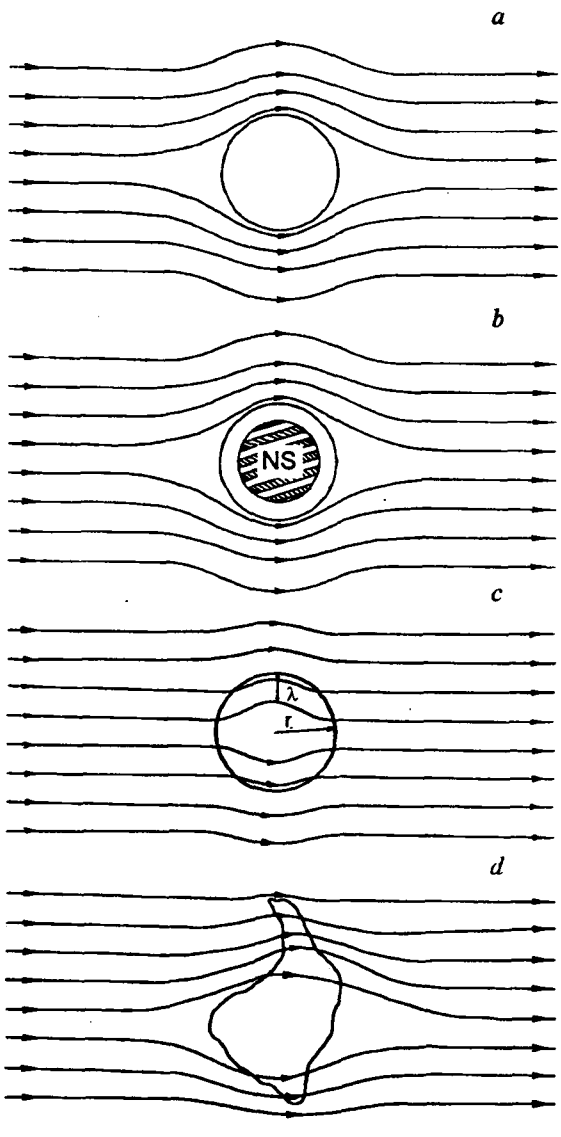


*Fig. 6.* Schematic picture of the flux expulsion from type II superconductors. Perfect superconductor of dimension $r$ much bigger than the penetration depth $\lambda$ (*a*); sample in the normal state (dashed region) with a superconducting surface layer (*b*); perfect superconductor of dimension $r$, which is of the order of the penetration depth $\lambda$ (*c*); nonideal geometry (*d*).

rity was discussed by Baenitz et al. [43,44]. The dependence of the diamagnetic response on the ratio $r/\lambda$ complicates the determination of the superconducting volume fraction.

In contrast to the ZFC case, field-cooled curves start with the flux uniformly distributed in the sample above $T_c$, and will show the Meissner effect at a certain temperature. This effect is masked by pinning in the system and can become almost zero in cases where pinning is very strong (see, for instance, Fig. 3,*a*). This means, that the FC susceptibility reveals the real $X_{sc}$ only in the ideal case of a perfect superconductor without structural defects, i.e. without pinning centers.

This implies that the evaluation of the superconducting fraction from the ZFC and FC curves is not correct. However, there is one further way to evaluate $X_{sc}$, i.e. from the slope of the linear dependence of $M$ on $H$ at $H < H_{c1}$. This method was used in Refs. 45 and 46 and appears to be better than the other ones. In this work, the shielding fraction $X_{sh}$, which has then to be corrected by $\lambda/r$ (see the next paragraph) to obtain the superconducting fraction $X_{sc}$, was evaluated at different temperatures from the measurement of the initial slope $\delta M/\delta H$ in the zero field cooling regime. Since in a perfect superconductor $M = -H$, the following definition for $X_{sh}$ was used: $X_{sh} = -\delta M/\delta H$. Low enough external fields ($H_{ext} \sim 1$ mT $\ll H_{c1}$) were applied. To take the demagnetizing factor $n$ into account, the samples were considered to be a set of independent superconducting spheres and the field inside the superconducting fraction was taken to be $H_{ext}/(1-n)$, $n = 1/3$ (see Refs. 45, 46 for details).

However, flux penetration between grains and the large penetration depth $\lambda$, which is close to the average grain size $r$, lead to flux penetration and pinning at fields below $H_{c1}$, and to a nonlinear $M(H)$ dependence. Such a nonlinearity was observed in almost all $M(H)$ measurements on fullerenes [40,42,45–49], which makes it difficult to obtain the slope $\delta M/\delta H$ for the $X_{sc}$ estimation and complicates the evaluation of $H_{c1}$ from these measurements (see Sec. 2). In addition, it is almost impossible to evaluate the exact magnitude of the demagnetizing factor $n$ due to the complex geometry of the particles. Their shapes are extremely irregular and the real dimensions are not well known.

From the above, it is clear that a quantitative evaluation of $X_{sc}$ is difficult for powdered samples and should be done very carefully. Almost all of the superconducting volume fractions published for fullerene superconductors were obtained from ZFC measurements. They vary between 40 and 90% in powder samples [25,26,48–51]. We believe that these values should be treated as a lower limit because of granularity effects.

## 2. Critical fields and characteristic lengths

As mentioned in the previous chapter, two fields, the lower critical field, $H_{c1}$, and the upper critical field, $H_{c2}$, are important for the characterization of a superconductor. Both fields can be determined from magnetization measurements. In order to evaluate the parameters, which are commonly used to characterize

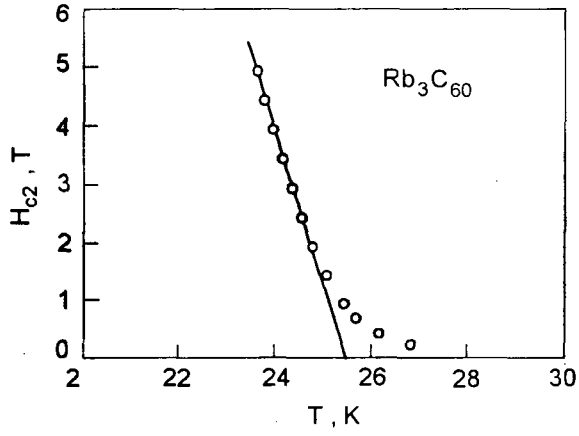


*Fig. 7.* Upper critical field $H_{c2}$ vs. temperature. The straight line corresponds to a slope $\mu_0 H' = -2.5$ T/K. (Reproduced from Ref. 45.)

the mixed state of type II superconductors, the Ginzburg–Landau relations [52] can be applied:

$$\mu_0 H_{c2} = \frac{\Phi_0}{2\pi \xi^2} , \qquad (1)$$

$$\mu_0 H_{c1} = \frac{\Phi_0}{4\pi \lambda^2} \ln \kappa , \qquad (2)$$

$$\kappa = \lambda / \xi . \qquad (3)$$

This approach is valid for all temperatures in the dirty limit.

### *2.1. Upper critical field and coherence length*

A large number of experiments was made to determine the upper critical field for crystalline [53–58] and powdered [33,40–42,44–46,48,59–63] fullerenes as well as for thin films [64] using different techniques such as magnetization [40–42,46,63], ac susceptibility [44,60], transport [62,64], rf absorption [61], etc. Almost all measurements were done on $K_3C_{60}$ and $Rb_3C_{60}$ and only one result is available on each of $RbCs_2C_{60}$ [63], $K_2CsC_{60}$ and $Rb_2CsC_{60}$ [65] and $Ba_6C_{60}$ [66]. Other superconducting fullerenes have not yet been characterized.

To obtain the temperature dependence of the upper critical field, $H_{c2}(T)$, from dc magnetization measurements, FC curves are usually used. One of the methods is when the critical temperature $T_c$ is determined from these experiments by the crossing point of the extrapolation of the linear part of the decreasing magnetization $M(T)$ in the superconducting state close to $T_c$, on the one hand, and the small normal-state magnetization, on the other hand. The upper critical field is equal to the applied external field, $H_{c2} = H_{ext}$. As an example, $H_{c2}(T)$, for a $Rb_3C_{60}$ sample, obtained in this way [45] is shown in Fig. 7. At temperatures not far below $T_c$, this dependence is linear except for fields $\mu_0 H < 1$ T, where a small «tail» is usually observed. The nature of this «tail» will be discussed below.

Due to the rather large values of $H_{c2}$ and the experimental limitation of the magnetic-field window (5–7 T in SQUID magnetometers) measurements of the upper critical field are usually performed at temperatures close to the transition temperature. The extrapolation of $H_{c2}(T)$ to zero is subject to a large uncertainty and depends on the fitting scheme. The standard theory by Werthamer—Helfand—Hohenberg (WHH) [67] is usually employed. This theory predicts $H_{c2}(T)$ dependence which follows roughly a power law $h = 0.6(1 - t^{\alpha})$, where $t \approx T/T_c$ and $\alpha \approx 1.75$ $H_{c2}(0)$ can be evaluated from the slope, $H'_{c2}$, of the linear dependence near $T_c$ by the relation

$$\mu_0 H_{c2}(0) = 0.69 T_c \frac{|d\mu_0 H_{c2}|}{dT}\Big|_{T_c} . \qquad (4)$$

In order to verify the applicability of this relation to $C_{60}$-based materials, several experiments were performed, in which $H_{c2}$ was measured at high magnetic fields [59–61]. Good agreement of the experimental data with the WHH prediction was obtained [59,61] demonstrating that this theory is successful in describing fullerene superconductors (Fig. 8). However, Boebinger et al. [60], who performed measurements on $K_3C_{60}$ powder, found an enhancement of $H_{c2}(T)$ compared to the theory. The authors proposed that the deviations could be attributed to flux motion in the superconducting powder, although other intrinsic mechanisms may also play a role. Additional enhancements of $H_{c2}$ at low temperatures could result from strong electron-phonon coupling which can lead to a relatively large increase in $H_{c2}(0)$, such that the temperature dependence of $H_{c2}$ becomes roughly linear [68]. Fermi-surface anisotropy [69] can also result in low-temperature enhancements of the upper critical field. Another mechanism proposed by the authors, which we consider to be more likely, is the dirty limit effect.

In the dirty limit, the Ginzburg–Landau coherence length $\xi_{GL}$ is expected to be limited by the mean free path $l$, $\xi_{GL} \sim (\xi_0 l)^{1/2}$, where $\xi_0$ is the BCS coherence length. Thus, in $C_{60}$-based superconductors, high upper critical fields might partly result from a reduction of $l$ [60] by different types of defects. One of them could be orientational disorder between adjacent $C_{60}$ molecules [70].

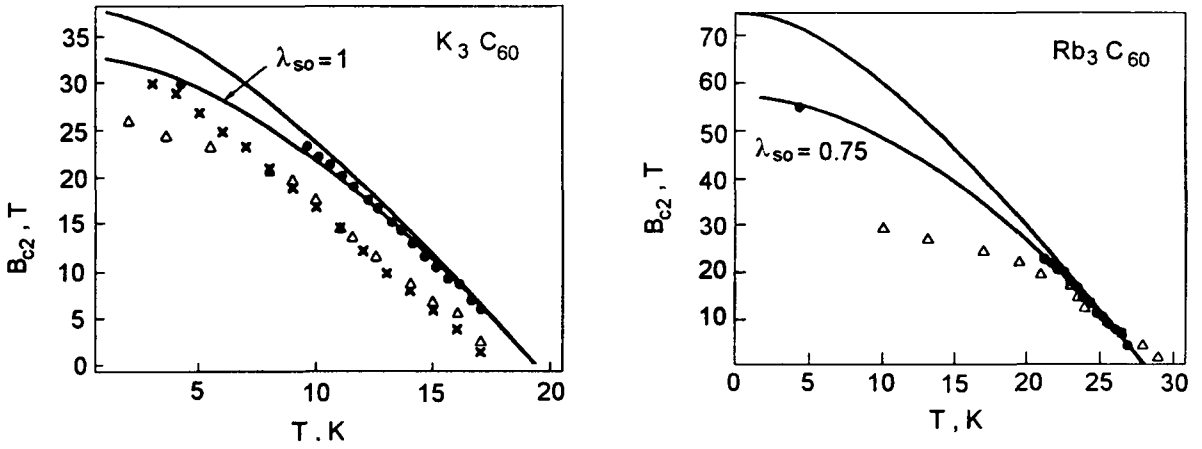


*Fig. 8.* The upper critical field vs. temperature for $K_3C_{60}$ powder (*a*) and $Rb_3C_{60}$ powder (*b*). The low field data are taken in dc fields and the data points at 4.2 K are taken in pulsed fields. The solid curves are fits to the data ( ● ) including Pauli paramagnetic limiting and the upper curves assume no paramagnetic limiting. Both experimental dependences follow roughly the WHH prediction [67]. (Reproduced from Ref. 61.)

This limitation of the mean free path could be the reason for the strong discrepancy between the experimentally obtained values of $H_{c2}(0)$ and $H'_{c2}$ (see Table 1). For example, for $K_3C_{60}$ $H'_{c2}$ varies from–2 to –5.5 T/K and for $Rb_3C_{60}$ from–2 to –3.9 T/K. This explanation could also be valid for the recently obtained very small value, $H'_{c2}$= –0.8 T/K, for $RbCs_2C_{60}$ [46].

From the values of $H_{c2}(0)$, the coherence length $\xi$ can be calculated using Eq. (1). Despite a large scatter (Table 1), which arises from the large scatter of

Table 1

Experimentally obtained mixed state parameters of fullerene superconductors. The data listed in the Table were obtained on crystalline [53–58], powder [33,40–42,44–46,48,59–63,65,66] and thin film [64] samples.

| Compound | $T_c$, K | $H_{c1}(0)$, mT | $H_{c2}(0)$, T | $-H'_{c2}$, T/K | $\lambda$, nm | $\xi$, nm | $\chi$ |
|---|---|---|---|---|---|---|---|
| $K_3C_{60}$ | 18.5 [60] | 13.2 [40] | 17.0 [44] | 1.40 [44] | 240 [89] | 2.0 [89] | 92 [40] |
| | 19.0 [84] | | 17.5 [84] | 1.34 [54] | 240 [40] | 2.6 [40] | 53 [54] |
| | 19.3 [28] | | 28.0 [59] | 2.00 [59] | 480 [83] | 2.9–3.3 [60] | |
| | 19.5 [61] | | 30–38 [60] | 2.14 [60] | 240 [54] | 3.4 [59] | |
| | 19.7 [54] | | 38 [61] | 2.18–2.8 [62] | | 4.4 [44] | |
| | | | 47 [64] | 2.80 [61] | | 4.5 [54] | |
| | | | 49 [40] | 3.50 [32] | | | |
| | | | | 3.73 [40] | | | |
| | | | | 5.5 [64] | | | |
| $Rb_3C_{60}$ | 27.5 [41] | 9–11.4 [45] | 40 [59] | 2.0 [59] | 320 [56] | 2.0 [42] | 80.5 [47] |
| | 28 [19] | 12 [42] | 44 [45] | 2.5 [45] | 240–280 [45] | 2.3 [45] | 104–122 [45] |
| | 29 [30,84] | 16.2 [47] | 44 [44] | 2.3 [44] | 215 [47] | 2.4 [56] | 123 [42] |
| | 29.4 [28] | | 46.5 [41] | | 247 [42] | 2.7 [41,44] | |
| | 30 [56] | | 62 [56] | 3.28 [56] | | 3.0 [59] | |
| | | | 76 [61] | 3.86 [61] | | | |
| | | | 78 [42] | 3.9 [42] | | | |
| $RbCs_2C_{60}$ | 33 [24,30,46] | 81 [46] | 0.8 [46] | 17 [46] | 300 [46] | 4.4 [46] | 68 [46] |
| $Ba_6C_{60}$ | 7 [26,66] | 13 [66] | 0.45 [66] | 2.2 [66] | 180 [66] | 12.0 [66] | 15 [66] |

$H_{c2}(0)$, it is clearly seen that the coherence length of fullerene superconductors is very small (tens of nanometers) and comparable to the short $\xi$ of high-$T_c$ superconductors.

One further interesting effect we would like to discuss here briefly, is the upturn of $H_{c2}(T)$ at temperatures very close to $T_c$. This upturn was observed in almost all experiments on all superconducting compounds [40,41,44,45,48,54,56,60,65,71]. Different authors suggested different explanations for this effect. In Ref. 40 the authors consider this deviation to be a consequence of slight variations in the local $T_c$, while in Ref. 44 the effect is attributed to a crossover from 3- to 2-dimensionality. One explanation [64], less interesting from the physics point of view, is that the upturn at low fields might be due to sample imperfections. In our opinion, this explanation is not very likely because the effect has been seen in samples with superconducting fractions from 1 to 75%, i.e. with very different quantities of imperfections. However, this would have to be checked by measurements on a sample of good quality. We propose that the upturn can be a consequence of the anisotropy of the Fermi surface of fullerene superconductors [69]. Strong effects of the anisotropy on magnetic properties of the conventional superconductors, specifically on the $H_{c2}(T)$ dependence, are well known [72]. The Fermi surface anisotropy exists also in fullerene superconductors inspite of their cubic lattice structure. Indeed, it was shown in Refs. 73 and 74 that an external magnetic field can lead to the appearance of Fermi surface anisotropy in metals with a cubic symmetry as a consequence of the strong anisotropy of microscopic properties. Anisotropy effects in the magnetic properties of superconducting niobium were analyzed in Ref. 75, and very good agreement between theory and experiment was found.

### 2.2. *Lower critical field and penetration depth*

More than ten different methods are available for measuring $H_{c1}$. Some of them are listed in the following: 1. methods involving the reversible magnetization at intermediate and high external magnetic fields; 2. the first deviation from the linear $M(H)$ behavior; 3. a method based on Bean's critical state model; 4. a method based on the magnetic field dependence of $\lambda$; 5. rf methods; 6. the torque method; 7. the mechanical-oscillator method; 8. the $\mu$SR and EPS methods; 9. a method involving an optical visualization of flux penetration; etc. All of these methods require a model for the evaluation of $H_{c1}$. In such a situation, the reliability of the results depends substantially on how well the relationship between $H_{c1}$ and the measured quantities can be established.

The first values of $H_{c1}$ for $K_3C_{60}$ [40], $Rb_3C_{60}$ [41,42], $RbCs_2C_{60}$ [46], and $Ba_6C_{60}$ [66] were obtained by a dc magnetization technique. $H_{c1}(0)$ evaluated from these measurements lies in the range $\mu_0 H_{c1} = 10$–$16$ mT (see Table 1). The temperature dependence of $H_{c1}$ can be described well by $H_{c1}(T)/H_{c1}(0) = 1 - (T/T_c)^2$ [40] and an example of this dependence [47] is shown in Fig. 9. From $H_{c1}(0)$ the penetration depth $\lambda$ is evaluated using Eq. (2) and the value of the coherence length known from independent measurements (Sec. 2.1). The magnitude of $\lambda$ obtained in this way is of the order of 200–250 nm (Table 1).

In these experiments the lower critical field was evaluated as the field at which a deviation from the linear $M(H)$ magnetization first appeared. Indeed, an ideal superconductor of spherical shape exhibits linear $M(H)$ behavior until $H_{c1}$, where a sharp cusp occurs. However, none of the magnetization data for fullerene materials show good linearity and no cusps. (The nature of such a behavior is discussed in Ref. 76.) $M(H)$ usually has a smooth positive (in some experiments even a negative) curvature. It is extremely difficult to obtain the point of first deviation from such a curve, since the deviations themselves are very small.

In order to make this procedure more quantitative, it is tempting to apply Bean's critical state model [77] for the entry of vortices into hysteretic superconductors. According to this theory, the magnetization is related to the critical current density $J_c$ (which is assumed to be field independent for simplicity), at fields above $H_{c1}$ by $(M + H) \sim (H_a^2 - H_{c1}^2)/J_c D$, where $D$ is a characteristic length for the sample

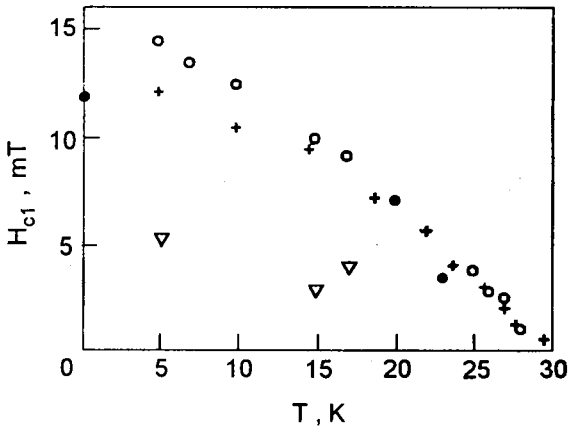


*Fig. 9.* Lower critical field $H_{c1}$ vs. temperature. ○ — Buntar et al. [47]; + — Sparn et al. [42]; ● — Politis et al. [45]. Triangles — data, obtained in Ref. 47 using Bean's critical state model. (Reproduced from Ref. 47.)

geometry studied. This relation holds in the range $H_{c1} < H < H^*$, where $H^* \sim J_c D$ is the field at which the flux penetrates the sample completely. Thus, a plot of $\delta M$ vs. $H^2$, where $\delta M = M + H_a$ is the deviation of the observed magnetization from perfect diamagnetic behavior, should give the lower critical field. This analysis was done for $Rb_3C_{60}$ [47] and $RbCs_2C_{60}$ [46]. In Ref. 46 these data agreed well with the data obtained from the first deviation from a linear dependence. However, both methods led to extremely high values of $H_{c1}$ at low temperatures and did not exhibit the «intrinsic» value of the lower critical field. In Ref. 47, the data obtained with Bean's analysis showed much smaller values of $H_{c1}$, (triangles in Fig. 9) and the authors related that to the field, at which breaking of intergranular Josephson junctions occurs.

The two above methods obviously do not lead to satisfactory results. Therefore, Politis et al. [45] and Buntar et al. [46] used an analysis, which is based on measurements of the reversible magnetization at high external fields and calculated $H_{c1}$ from the well known relations [78]

$$-M = \frac{H_{c2}(T) - H}{(2\kappa^2 - 1)\beta_a}; \qquad -M = \frac{\alpha\Phi_0}{8\pi\lambda^2(T)} \ln\frac{\beta H_{c2}(T)}{H} \tag{5}$$

for high and intermediate magnetic fields, respectively. This analysis led to values of the lower critical field, which were slightly smaller but comparable to the data obtained by the first two methods [45,46].

The last method being based on direct measurements of the reversible magnetization is more accurate for the determination of the lower critical field. However, the resulting calculated values of the Ginzburg–Landau parameter $\kappa$ and, hence, of $H_{c1}$ strongly depend on the value of the superconducting fraction assumed (see Ref. 46, Eq. (4)) and this leads to an enormous uncertainty in quantitative calculations, especially in the case of powdered samples with a large distribution of grain sizes.

In order to avoid the difficulties arising from the previous three methods, another way to evaluate $H_{c1}$ must be found. In our recent investigations we used a method developed by Böhmer [79], in which $H_{c1}$ is determined through measurements of the trapped magnetization. This method is far more accurate than the measurements of $\delta M$, because of the cancellation of a large linear contribution [80]. It is based on the fact that trapped magnetic flux, $M_t$, can be built up in a sample only when the field had been increased beyond $H_{c1}$. The advantage of this method for type II superconductors with strong pinning was illustrated in Ref. 80, where the $M(H)$ behavior was shown to appear quite linear in the vicinity of $H_{c1}$, whereas $M_t^{1/2}$ vs. $H$ showed a well-resolved kink at the field corresponding to $H_{c1}$.

We performed such measurements on $RbCs_2C_{60}$ powder and on crystalline $Rb_3C_{60}$ and $K_3C_{60}$ samples. The magnetic field dependence of $M_t$ at $T = 5$ K for the $Rb_3C_{60}$ sample is shown in Fig. 10. The demagnetization factor $n$ is taken to be 1/3 for the $Rb_3C_{60}$ sample, because the shape of the crystal is roughly spherical, and for the $RbCs_2C_{60}$ sample, because the powder can be approximated by a set of independent spheres. For the $K_3C_{60}$ sample, which has the shape of a narrow plate, $n = 0$.

As expected, at small fields, $H < H_t$, there is no trapped magnetization, $M$ has a background value and is field independent. At some characteristic field $H_t$ a well-resolved kink is clearly seen. When the magnetic field exceeds $H_t$, a trapped magnetization appears and increases with increasing external field. The $M_t(H)$ dependence follows $M_t^{1/2} \sim H$ as predicted in Ref. 80. The very unexpected result is that the values of $H_t$ are very small in comparison with values of $H_{c1}$ obtained previously from $\delta M$ measurements. $H_t$ could be related to intergranular effects. However, breaking the intergranular coupling does not lead to such a strong trapped flux. We propose that $H_t$ is the lower critical field of fullerene superconductors.

All our previous knowledge on the lower critical field of fullerenes was based on results where $H_{c1}$ was obtained from $\delta M$ measurements which are not very precise. The $M(H)$ dependence in these measure-

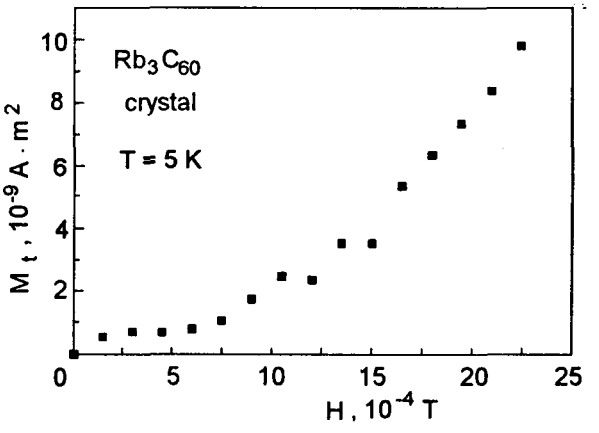


*Fig. 10.* Magnetic field dependence of the trapped magnetization $M_t$ at $T = 5$ K for $Rb_3C_{60}$ crystal.

ments did not exhibit any linearity, which could be related to the fact that the measurements were performed at field-steps of 0.5 or 1 mT.

Small values of the field at which the trapped magnetization appeared, similar to our results, were also observed by Kraus [81] by measuring the irreversible $M(T)$ curves. Additionally, in several publications small values of the penetration field were obtained [47,82], but attributed to breaking intergranular coupling. Moreover, in more direct measurements of $\lambda$ [83] by $\mu$SR experiments the penetration depth was found to be 480 nm for $K_3C_{60}$ and 420 nm for $Rb_3C_{60}$, which leads to $H_{c1}(0) = 4.0$ mT and 4.9 mT, respectively. All these data compel us to undertake more detailed and careful investigations of the lower critical field in fullerenes.

## Conclusions

In the present contribution, an attempt was made to highlight some experimental results on the magnetization of crystalline and powdered fullerene superconductors and to emphasize the role of these experiments in achieving an improved insight into the physics of fullerene superconductivity.

We did not discuss interesting results on the hysteretic properties of the magnetization and the evaluation of the critical current density [40–42,63] and the irreversibility line [84,85], the time-relaxation of the irreversible magnetization [41,86] as well as the results on the pinning mechanisms in fullerene superconductors [87,88].

Our discussion of experimental results from magnetic measurements may be summarized as follows.

Only two superconducting fullerenes, $K_3C_{60}$ and $Rb_3C_{60}$, have been characterized by several groups. Only one measurement of the critical fields and the characteristic lengths has been performed for the compounds $RbCs_2C_{60}$ [46], $Ba_6C_{60}$ [66] and sodium-doped $C_{60}$ [48]. No other fullerene superconductors have yet been characterized.

The values of $H_{c2}$ vary widely from sample to sample, while the values of $H_{c1}$ cannot be compared because only one or two data points exist for each compound as mentioned in the previous paragraph. Moreover, the values of $H_{c1}$ deduced from these experiments seem to be overestimated.

In conclusion, we wish to point out that the effects of granularity in powdered samples and the possible granularity of bulk crystals represent a central problem because one must know whether the parameters obtained from experiments are characteristic of bulk material or of weak links in order to establish the intrinsic superconducting parameters of new superconductors. We believe that with the increasing quality of single crystals, significant progress towards a better understanding of the mixed state properties lies immediately ahead, and that magnetization measurements and their comparison with other techniques will play a key role in this development.

## Acknowledgments

We thank Prof. J. E. Fischer (University of Pennsylvanya), Prof. H. Kuzmany (University of Vienna) and Prof. M. Ricco (Parma University) for providing us with the samples used for the measurements described in Sec. 2.2. We are grateful to our colleagues from the Low Temperature Laboratory, Atominstitut, for help with the experiments. This work was supported by the Fonds zur Förderung der Wissenschaftlichen Forschung, Wien.

1. E. A. Rohlfing, D. M. Cox, and A. Kaldor, *J. Chem. Phys.* **81**, 3322 (1984).
2. H. W. Kroto, J. R. Heath, S. C. O'Brein, R. F. Curl, and R. E. Smalley, *Nature* **318**, 162 (1985).
3. W. Krätschmer, L. D. Lamb, K. Fostiropoulos, and D. R. Huffman, *Nature* **347**, 345 (1990).
4. J. E. Fischer and P. A. Heiney, *J. Phys. Chem. Solids* **54**, 1725 (1993).
5. P. A. Heiney, *J. Phys. Chem. Solids* **53**, 1333 (1992).
6. K. Prassides, H. W. Kroto, R. Taylor, D. R. M. Walton, W. I. B. David, J. Tomkinson, R. C. Haddon, M. J. Rosseinsky, and D. W. Murphy, *Carbon* **30**, 1277 (1993).
7. R. M. Fleming, T. Siegrist, P. M. Marsh, B. Hessen, A. R. Kortan, D. W. Murphy, R. D. Haddon, R. Tycko, G. Dabbagh, A. M. Mujsce, M. L. Kaplan, and S. M. Zahurak, *MRS Symp. Proc.* 206: *Clusters and Cluster-Assembled Materials*, R. S. Averback, J. Bernholc, and D. L. Nelson (eds.), MRS, Pittsburg (1991).
8. P. A. Heiney, J. E. Fischer, A. R. McGhie, W. J. Romanow, A. M. Denenstein, J. P. McCauley, and A. B. Smith III, *Phys. Rev. Lett.* **66**, 2911 (1991).
9. R. A. Sachidanadan and A. B. Harris, *Phys. Rev. Lett.* **67**, 1467 (1991).
10. A. Dworkin, H. Szware, S. Leach, J. P. Hare, T. J. Dennis, H. W. Kroto, R. Taylor, and D. R. M. Walton, *C. R. Acad. Sci. Paris-Serie II*, bf **312**, 979 (1991).
11. W. I. F. David, R. M. Ibberson, T. J. S. Dennis, J. P. Hare, and K. Prassides, *Europhys. Lett.* **18**, 219 (1992).
12. W. I. F. David, R. M. Ibberson, T. J. S. Dennis, J. P. Hare, and K. Prassides, *Europhys. Lett.* **18**, 735 (1992).
13. R. C. Yu, N. Tea, M. B. Salamon, D. Lorents, and R. Malhotra, *Phys. Rev. Lett.* **68**, 2050 (1992).
14. V. I. Zubov, N. P. Tretiakov, J. N. Teixeira Rabelo, and J. F. Sanches Ortiz, *Phys. Lett.* **A194**, 223 (1994).
15. R. C. Haddon and V. Elser, *Chem. Phys. Lett.* **169**, 362 (1990).
16. R. S. Ruoff, D. Beach, J. Cuomo, T. McGuire, R. L. Whetten, and F. Diederich, *J. Phys. Chem.* **91**, 3457 (1991).
17. R. C. Hadon, A. F. Hebbard, M. J. Rosseinsky, D. W. Murphy, S. J. Duclos, K. B. Lyons, B. Miller, J. M. Rosamilia, R. M. Fleming, A. R. Kortan, S. H. Glarum, A. V. Makhija, A. J. Miller, R. H. Elck, S. M. Zahurak, R. Tycko, G. Dabbagh, and F. A. Thiel, *Nature* **350**, 320 (1991).
18. A. F. Hebard, M. J. Rosseinsky, R. C. Haddon, D. W. Murphy, S. H. Glarum, T. T. M. Palstra, A. P. Ramirez, and A. R. Kortan, *Nature* **350**, 600 (1991).
19. M. J. Rosseinsky, A. P. Ramirez, S. H. Glarum, D. W. Murphy, R. C. Haddon, A. F. Hebard, T. T. M. Palstra, A. R. Kortan, S. M. Zahurak, and A. V. Makhija, *Phys. Rev. Lett.* **66**, 2830 (1991).

20. R. F. Curl and R. E. Smalley, *Scientific America* 32, October (1991).
21. J. G. Bednorz and K. A. Müller, *Z. Phys.* B64, 189 (1986).
22. C. W. Chu, P. H. Hor, R. L. Meng, et al., *Phys. Rev. Lett.* 58, 405 (1987).
23. T. T. M. Palstra, O. Zhou, Y. Iwasa, P. E. Sulewski, R. M. Fleming, and B. R. Zegarski, *Solid State Commun.* 93, 327 (1995).
24. K. Tanigaki, I. Hirosawa, T. W. Ebbesen, J.-I. Mizuki, and J.-S. Tsai, *J. Phys. Chem. Solids* 54, 1645 (1993).
25. P. W. Stephens, L. Mihaly, P. L. Lee, R. L. Whetten, S.-M. Huang, R. Kaner, F. Diederich, and K. Holtzer, *Nature* 351, 632 (1991).
26. A. R. Kortan, N. Kopylov, S. Glarum, E. M. Gyorgy, A. P. Ramirez, R. M. Fleming, O. Zhou, F. A. Thiel, P. L. Trevor, and R. C. Haddon, *Nature* 360, 566 (1992).
27. A. R. Kortan, N. Kopylov, S. Glarum, E. M. Gyorgy, A. P. Ramirez, R. M. Fleming, F. A. Thiel, and R. C. Haddon, *Nature* 355, 529 (1992).
28. R. M. Fleming, A. P. Ramirez, M. J. Rosseinsky, D. W. Murphy, R. C. Haddon, S. M. Zahurak, and A. V. Makhija, *Nature* 352, 787 (1991).
29. O. Zhou et al., *Science*, 255, 833 (1992).
30. K. Tanigaki, I. Hirosawa, T. W. Ebbesen, J. Mizuki, Y. Shimakawa, Y. Kubo, J. S. Tsai, and S. Kuroshima, *Nature*, 356, 419 (1992).
31. A. Oshiyama and S. Saito, *Solid State Commun.* 82, 41 (1992).
32. A. P. Ramirez, M. J. Rosseinsky, D. W. Murphy, and R. C. Haddon, *Phys. Rev. Lett.* 69, 1687 (1992).
33. R. Tyco et al., *Science* 253, 884 (1991).
34. J. E. Schirber et al., *J. Phys. Chem. Solids* 54, 1427 (1993).
35. K. Kniaz, J. E. Fischer, Q. Zhu, M. J. Rosseinsky, O. Zhou, and D. W. Murphy, *Solid State Commun.* 88, 47 (1993).
36. K. Prassides, C. Christides, I. M. Thomas, J. Mizuki, K. Tanigaki, I. Hirosawa, and T. W. Ebbesen, *Science* 263, 950 (1994).
37. T. Yildirim, J. E. Fischer, R. Dinnebier, P. W. Stephens, and C. L. Lin, *Solid State Commun.* 93, 269 (1995).
38. T. Yildirim, J. E. Fischer, A. B. Harris, P. W. Stephans, D. Liu, L. Brard, R. M. Strongin ,and A. B. Smith III, *Phys. Rev. Lett.* 71, 1383 (1993).
39. M. P. Gelfand, *Superconductivity Review* 1, 103 (1993).
40. K. Holczer, O. Klein, G. Grüner, J. D. Thompson, F. Diederich, and R. L. Whetten, *Phys. Rev. Lett.* 67, 271 (1991).
41. C. Politis, V. Buntar, W. Krauss, and A. Gurevich, *Europhys. Lett.* 17, 175 (1992).
42. G. Sparn, J. D. Thompson, R. L. Whetten, S.-M. Huang, R. B. Kaner, F. Diederich, G. Grüner, and K. Holtzer, *Phys. Rev. Lett.* 68, 1228 (1992).
43. A. I. Sokolov, Yu. A. Kufaev, and E. B. Sonin, *Physica* C212, 19 (1993).
44. M. Baenitz, M. Heinze, E. Straube, H. Werner, R. Schlögl, V. Thommen, H.-J. Güntherodt, and K. Lüders, *Physica* C228, 181 (1994).
45. C. Politis, A. I. Sokolov, and V. Buntar, *Mod. Phys. Lett.* B6, 351 (1992).
46. V. Buntar, M. Ricco', L. Cristofolini, H. W. Weber, and F. Bolzoni, *Phys. Rev.* B (1995) (in press).
47. V. Buntar, U. Eckern, and C. Politis, *Mod. Phys. Lett.* B6, 1037 (1992).
48. I. I. Khairullin, K. Imaeda, K. Yakushi, and H. Inokuchi, *Physica* C231, 26 (1994).
49. V. A. Stenger, C. H. Pennington, D. R. Buffinger, and R. P. Ziebarth, *Preprint. Nuclear magnetic resonance of* $A_3C_{60}$ *superconductors* (1995).
50. M. Tokumoto, Y. Tanaka, N. Kinoshita, T. Kinoshita, S. Ishibashi, and H. Ihara, *J. Phys. Chem. Solids* 54, 1667 (1993).
51. K. Imaeda, I. I. Khairullin, K. Yakushi, and H. Inokuchi, *Proc. of ICSM'94 (Seoul)*, Synth. Metals, (in press).
52. P. G. deGennes, *Superconductivity of Metals and Alloys*, W. A. Benjamin INC., New York - Amsterdam (1966).
53. H. Ogata, T. Inabe, H. Hoshi, Y. Maruyama, Y. Achiba, S. Suzuki, K. Kikuchi, and I. Ikemoto, *Jpn. J. Appl. Phys.* 31, L166 (1992).
54. J. G. Hou, V. H. Crespi, X.-D. Xiang, W. A. Vareka, G. Briceno, A. Zettl, and M. L. Cohen, *Solid State Commun.* 86, 643 (1993).
55. X.-D. Xiang, J. G. Hou, G. Briceno, W. A. Vareka, R. Mostovoy, A. Zettl, V. H. Crespi, and M. L. Cohen, *Science* 256, 1190 (1992).
56. J. G. Hou, X.-D. Xiang, V. H. Crespi, M. L. Cohen, and A. Zettl, *Physica* C228, 175 (1994).
57. C. Gu, B. W. Veal, R. Liu, A. P. Paulikas, P. Kostic, H. Ding, K. Gofron, J. C. Campuzano, J. A. Schlueter, H. H. Wang, U. Geiser, and J. M. Williams, *Phys. Rev.* B50, 16566 (1994).
58. V. Buntar et al., (to be published).
59. C. E. Johnson, H. W. Jiang, K. Holtczer, R. B. Kaner, R. L. Whetten, and F. Diederich, *Phys. Rev.* B46, 5880 (1992).
60. G. S. Boebinger, T. T. M. Palstra, A. Passner, M. J. Rosseinsky, and D. W. Murphy, *Phys. Rev.* B46, 5876 (1992).
61. S. Foner, E. J. McNiff, D. Heiman, S.-M. Huang, and R. B. Kaner, *Phys. Rev.* B46, 14936 (1992).
62. J. G. Hou, X.-D. Xiang, M. L. Cohen, and A. Zettl, *Physica* C232, 22 (1994).
63. C. Politis, V. Buntar, and V. P. Seminozhenko, *Intern. J. Mod. Phys.* B7, 2163 (1993).
64. T. T. M. Palstra, R. C. Haddon, A. F. Hebard, and J. Zaanen, *Phys. Rev. Lett.* 68, 1054 (1992).
65. M. Baenitz, M. Heinze, K. Lüders, H. Werner, and R. Schlögl, *Proc. of IWEP'95* (Kirchberg, Tirol), World Scientific Publishing Ltd., (in press).
66. V. Korenivski, K. V. Rao, and Z. Iqbal, *Phys. Rev.* B50, 13890 (1994).
67. N. R. Werthamer, E. Helfand, and P. C. Hohenberg, *Phys. Rev.* 147, 295 (1966).
68. J. P. Carhotte, *Rev. Mod. Phys.* 62, 1027 (1990).
69. S. C. Erwin and W. E. Pickett, *Science* 254, 842 (1991).
70. M. P. Gelfand and J. P. Lu, *Phys. Rev. Lett.* 68, 1050 (1992).
71. M. Baenitz, M. Heinze, K. Lüders, H. Werner, and R. Schlögl, *Solid State Commun.* 91, 337 (1994).
72. *Anisotropy Effects in Superconductors*, H. W. Weber (ed.), Plenum Press, New York (1977).
73. V. V. Marchenkov, A. N. Cherepanov, V. E. Startsev, C. Czurda, and H. W. Weber, *J. Low Temp. Phys.* 98, 425 (1995).
74. V. V. Marchenkov, H. W. Weber, A. N. Cherepanov, and V. E. Startsev, *J. Low. Temp. Phys.* (to be published).
75. H. W. Weber, E. Seidl, C. Laa, E. Schachinger, M. Prohammer, A. Junod, and D. Eckert, *Phys. Rev.* B44, 7585 (1991).
76. A. P. Ramirez, *Supercond. Rev.* 1, 1 (1994).
77. C. P. Bean, *Phys. Rev. Lett.* 8, 250 (1962).
78. A. A. Abrikosov, *Zh. Eksp. Teor. Fiz.* 32, 1442 (1957).
79. C. Böhmer, *The lower critical field in high-*$T_c$ *single crystals*, Ph. D. Thesis, Atominstitut der Österriechischen Universitäten, Vienna (1995).
80. V. Moshchalkov, J. V. Henry, C. Marin, J. Rossat-Mignod, and J. F. Jacquot, *Physica* C175, 407 (1991).
81. M. Kraus, H. Sindlinger, H. Werner, R. Schlögl, V. Thommen, H. P. Lang, H.-J. Cütherodt, and K. Lüders, *J. Phys. Chem. Solids, Proc. of 8th ISIC*, Vancouver, Canada (1995).
82. J. D. Thompson, G. Sparn, K. Holczer, O. Klein, G. Crüner, R. B. Kaner, F. Diederich, and R. L. Whetten, in: *Physical and Material Properties of High Temperature Superconductors*, S. K. Malic and S. S. Shah, (eds.), p. 139, Nova Science Publishers, Commack, NJ (1994).
83. Y. J. Uemura, A. Keren, L. P. Le, G. M. Luke, B. J. Sternlieb, W. D. Wu, J. H. Brewer, R. L. Whetten, S. M. Huang, S. Lin, R. B. Kaner, F. Diederich, S. Donovan, G. Crüner, and K. Holtzer, *Nature* 352, 606 (1991).
84. C. L. Lin, T. Mihalisin, N. Bykovetz, Q. Zhu, and J. E. Fischer, *Phys. Rev.* B49, 4285 (1994).

85. V. Buntar, M. Ricco, L. Cristofolini, M Grassi, and F. Bolzoni, in: *Proc. of IWEP'95* (Kirchberg, Tirol), World Scientific Publishing Ltd (in press).
86. C. L. Lin, T. Mihalisin, M. M. Labes, N. Bykovetz, Q. Zhu, and J. E. Fischer, *Solid State Commun.* 90, 629 (1994).
87. V. Buntar, *Phys. Lett.* A184, 131 (1993).
88. V. Buntar and A. G. Buntar, *Phys. Rev.* B51, 1311 (1995).
89. W. H. Wong, M. E. Hanson, W. G. Clark, G. Grüner, J. D. Thompson, R. L. Whetten, S.-M. Huang, R. B. Kaner, F. Diederich, P. Petit, J.-J. Andre, and K. Holtzer, *Europhys. Lett.* 18, 79 (1992).
90. M. Mizuki et al., Phys. Rev. B50, 3466 (1994).